ELSEVIER

Journal of Nuclear Materials 313–316 (2003) 56–61

journal of nuclear materials

www.elsevier.com/locate/jnucmat

Deuterium bombardment of carbon and carbon layers on titanium

K.U. Klages, A. Wiltner, J. Luthin, Ch. Linsmeier *

Max-Planck-Institut für Plasmaphysik, EURATOM Association, Boltzmannstrasse 2, D-85748 Garching b. München, Germany

Abstract

Interaction of deuterium ions with highly oriented pyrolytic graphite and thin carbon layers on titanium are studied by X-ray photoelectron spectroscopy (XPS) measurements. The effects induced by the deuterium beam are compared to bombardment with chemically inert argon ions. XPS allows the identification of several carbon states: graphitic carbon, disordered graphitic carbon, ion-induced radiation defects in carbon, and carbidic carbon in the carbon films on titanium. Erosion of the carbon film by deuterium proceeds through two paths: first a chemical erosion with a cross-section of 4.7×10^{-17} cm^2 removes elementary carbon. At the same time, carbidic carbon is eroded with a linear yield of 0.003 within the fluence range between 8×10^{16} and 1.4×10^{17} cm^{-2}.

PACS: 68.35.Dv; 79.20.Rf; 82.20.Pm; 82.80.Pv
Keywords: Carbon; Titanium; Carbide; Erosion; Surface effects; XPS

1. Introduction

The application of different materials for use as plasma-facing components (PFCs) at the first wall of modern fusion experiments [1] and in the design of ITER [2,3] leads to the formation of multi-component materials due to erosion, material transport through the plasma and redeposition of materials at different locations [4,5]. Elevated wall temperatures and energetic particles allow compound formation at the surfaces as well as diffusion of surface species into the bulk material [6,7]. Compound surface layers influence the hydrogen inventory in the PFCs by modifying the hydrogen isotope diffusion through these layers, the chemical erosion behavior of the PFC surface towards hydrogen, and the hydrogen adsorption and desorption properties of the surfaces.

In order to understand and consequently predict hydrogen isotope interactions with multi-component PFC materials it is necessary to comprehend the principal interaction mechanisms of hydrogen with pure and mixed PFC materials. In previous work we studied the surface interaction of carbon with several materials, leading to carbide formation and carbon diffusion at elevated temperatures [6,8–10]. We also demonstrated that the bombardment of carbon layers on Ti and W with chemically inert noble gas ions leads both to sputtering and formation of a carbide phase at the surface [11]. In this work, the interaction of deuterium ions in the keV energy regime with pure carbon, as well as with carbon films on titanium is studied by X-ray photoelectron spectroscopy (XPS). The results of the XPS measurements are compared to kinematic simulations of the ion–solid interactions using the Monte Carlo code TRIDYN [12] which describes dynamic compositional changes due to ion bombardment.

2. Experimental

Samples for this investigation are highly oriented pyrolytic graphite (HOPG ZYA, Advanced Ceramics), and a polycrystalline titanium foil (Goodfellow). Sample areas are approx. 1 cm^2 and thicknesses 1 mm. The

* Corresponding author. Tel.: +49-89 3299 2285; fax: +49-89 3299 2279.
E-mail address: linsmeier@ipp.mpg.de (Ch. Linsmeier).

0022-3115/03/$ - see front matter
PII: S0022-3115(02)01332-6

HOPG surface is stripped by adhesive tape before insertion into the ultra-high vacuum system (UHV, base pressure in the low 10^{-8} Pa range). XPS measurements performed directly after sample insertion show only signals originating from carbon; no further cleaning of the HOPG surface in UHV is applied prior to ion bombardment.

Titanium is mechanically polished to mirror-like finish. Cleaning under vacuum involves heating/sputtering cycles (970 K, 5 keV Ar^+) until only metal signals are detected by XPS. Carbon films on Ti are deposited from an Omicron EFM3 source using high-purity carbon (99.999%, Goodfellow). The chemical state of the sample surfaces is characterized using XPS with monochromatic AlKα radiation (PHI ESCA 5600). This technique is very suitable to distinguish carbon in its graphitic and carbidic phases [9]. Additional details regarding the analysis and sample preparation system can be found elsewhere [13].

The binding energies in the XPS spectra are referenced to the graphitic C 1s signal at 284.2 eV from the respective spectra. The analyzer work function is referenced to the Au $4f_{7/2}$ signal at 84.0 eV. Spectra are accumulated with a pass energy of 2.95 eV at an electron exit angle of 22° with respect to the surface normal. Ion bombardment is carried out using a non-mass separated ion source (Specs IQ 12/38). Ion fluences are calculated with known implantation areas at the sample surface and sample current measurements. For deuterium bombardment, fluences are calculated assuming D^+ ions, although D_2^+ and D_3^+ may as well be present.

3. Results

3.1. Graphite

An HOPG sample is bombarded with 1 keV D^+ ions up to fluences of 2.3×10^{16} cm^{-2}. Between ion bombardment cycles, XPS spectra are taken in survey and high resolution modes. Survey spectra prove no contamination accumulation at the sample surface during all treatment steps, since only peaks attributable to carbon are observed. Already after a D^+ fluence of 1×10^{15} cm^{-2} the C 1s peak shows a shift in its overall maximum of 0.1 eV to lower binding energies (from 284.2 to 284.1 eV). After 2.3×10^{16} cm^2, the shift amounts to 0.15 eV and after annealing at 700 K the peak maximum is at 284.0 eV. In contrast to Ar^+ bombardment measurements of thin carbon layers on gold [9] where the disorder introduced by the ion beam and the remaining graphitic peak can be separated unambiguously by peak fitting, this procedure is not successful here. Nonetheless, to gain information on the additionally introduced binding states of carbon under D^+ irradiation, the C 1s spectrum from clean, unirradiated HOPG is subtracted from the respective spectra after ion impact after Shirley background removal. The difference spectra are plotted in Fig. 1 in two groups for better visibility. The upper group consists of the first six implantation steps between 1.0 and 4.7×10^{15} cm^{-2}. The lower group comprises the following five implantation steps from 6.6 to 23×10^{15} cm^{-2} together with the final annealing experiment at 700 K for 30 min. Solid and broken lines alternate with increasing fluences, the first and last curves in the groups are marked in the plot. Positive intensity differences (values above the 0 lines) in these spectra denote additional intensity compared to clean HOPG, whereas negative values show decreased intensity at the respective energy.

The difference spectra immediately indicate intensity variations during the treatment cycles at three distinct binding energies. The intensity changes (height at maximum/minimum in Fig. 1) of the three peaks in the difference spectra are plotted with increasing deuterium fluence in Fig. 2(a). The largest changes take place at a binding energy (BE) of 284.2 eV, which we attribute to graphitic carbon. The position of this peak does not change throughout the whole treatment series. However, intensity in this position continuously decreases compared to the clean HOPG. After the final 700 K heating, a slight increase in intensity at this position is again observed. The peak at the higher BE of 284.9 eV is very weak, but also stable in position. Intensity at this BE

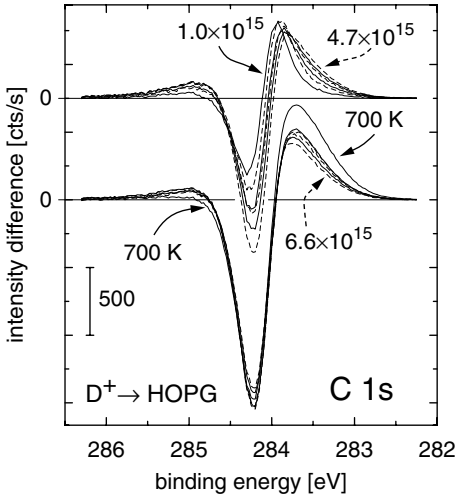

Fig. 1. XPS difference spectra in the C 1s region of HOPG bombarded with 1 keV D^+ ions. The consecutive fluence steps are separated into two groups. Successive spectra are marked with solid and broken lines, respectively. Some fluences are indicated, the intermediate fluences correspond to the values of the data points in Fig. 2. The final spectrum is measured after annealing at 700 K for 30 min.

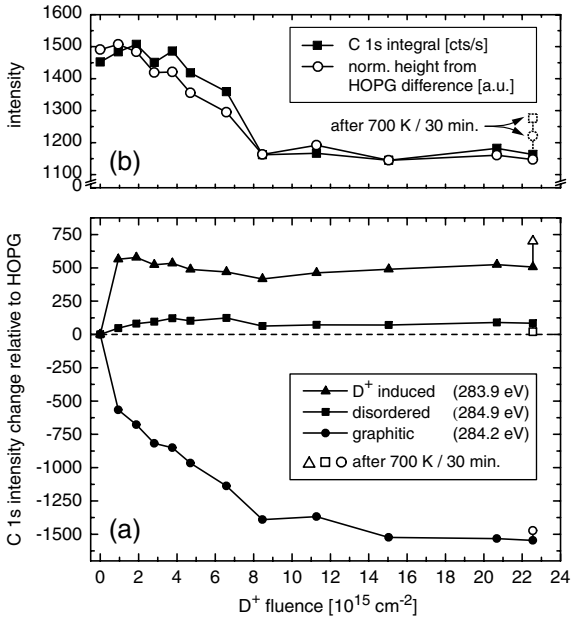

Fig. 2. Panel (a) shows the intensity changes of the three peaks identified in Fig. 1. Positive values indicate an increase in intensity compared to HOPG at the respective BE, negative values a decrease. Panel (b) compares the total C 1s intensity from the raw spectra (after subtraction of a Shirley background) with the sum of the heights from panel (a) at each fluence. The height curve is normalized to compare with the intensity curve. Values after 700 K heating are indicated in the plots.

increases during the first implantation steps up to approx. 7×10^{15} cm^{-2}. At higher fluences, first a small decrease is noticed and the intensity is then constant up to the final implantation step. After heating at 700 K, the intensity around 284.9 eV almost drops back to the level at the clean HOPG surface. The third peak component appears around 283.9 eV and shifts during the implantation to 283.7 eV. This component appears immediately after the first ion implantation step and maintains the initial maximum intensity throughout the subsequent ion treatments. It is only after the 700 K heating that the intensity of this component increases again and reaches a new maximum, while remaining constant at 283.7 eV BE.

A justification for this method of spectrum evaluation by differences is the overall development of the sum of the three difference peaks. In Fig. 2(b) the sum of the three peaks is plotted together with the total C 1s peak integral from the XPS spectra (after Shirley background subtraction). For comparison, the sum is normalized to the amplitude of the C 1s curve. Both lines show the same overall behavior: after a small initial intensity increase during the start of ion bombardment the curves decrease until a fluence of approx. 8×10^{15} cm^{-2} is

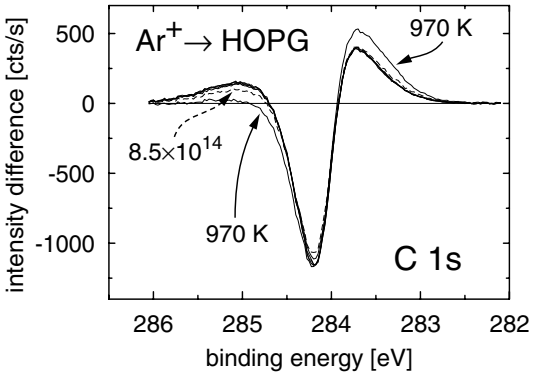

Fig. 3. XPS difference spectra in the C 1s region of HOPG bombarded with 1 keV Ar^+. Sample treatments are indicated. The overlapping spectra correspond to fluences from 2.1 to 8.5×10^{15} cm^{-2}, respectively.

reached. At higher fluences, no changes are observed. The intensity increase seen for the C 1s peak after sample heating to 700 K is also reproduced by the sum of the difference peaks.

The variations in the difference spectra of the HOPG bombarded with deuterium is compared to HOPG bombarded with argon. Fig. 3 shows an analogous experiment to Fig. 1 for 1 keV Ar^+ up to a fluence of 8.5×10^{15} cm^{-2} and final annealing to 970 K for 60 min. As in the difference spectra from the D^+ experiment, three peaks are observed. However, the peak positions after Ar^+ bombardment do not vary with fluence. The peak around 285 eV appears under Ar^+ bombardment and develops with fluence. The dashed line corresponds to 8.5×10^{14} cm^{-2}, the subsequent implantation steps (fluence of 2.1–8.5×10^{15} cm^{-2}) already show saturation at this BE. After annealing to 970 K this peak almost completely vanishes again, as in the deuterium case. The gradual changes with fluence are also visible in the intensity at 284.2 eV. At this position, however, no influence of the annealing step is recognized. The peak around 283.7 eV exhibits the most pronounced alteration after annealing. While Ar^+ bombardment creates this peak already after the first fluence step and subsequent implantation cycles do not modify it, annealing strongly increases the intensity at this BE. The peak position, however, remains unaffected.

3.2. Carbon films on titanium

A 2.9 nm carbon film on titanium is bombarded with 4 keV D^+ ions up to a fluence of 1.4×10^{17} cm^{-2}. Depending on the applied model for electron attenuation lengths is solids [14], it is several nm for our experimental parameters. The XPS information depth therefore is larger than the carbon layer thickness. Fig. 4 shows the C 1s range after the indicated fluences. The

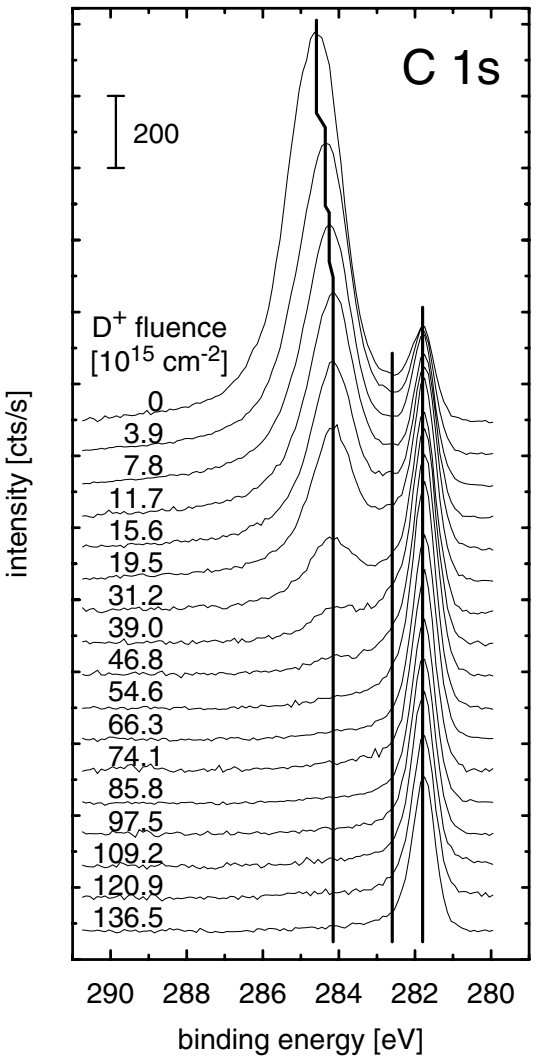

Fig. 4. XPS spectra in the C 1s region of a 2.9 nm carbon film on titanium before and after D^+ ion bombardment at 4 keV. The curves are labeled with the applied D^+ fluences. The vertical lines indicate binding energies of graphitic carbon (284.2 eV), titanium subcarbides (282.6 eV), and TiC (281.8 eV), respectively.

spectrum without ion bombardment shows a broad peak (compared to HOPG) located at 284.6 eV, originating from graphitic carbon. A second peak at 281.8 eV originates from TiC, formed at the interface between deposited carbon and titanium metal. Between these peaks, intensity is recorded around 282.6 eV, where titanium subcarbides are located. The graphitic peak shifts already after a fluence of 3.9×10^{15} cm^{-2} by 0.11 eV to lower binding energies and reaches a fixed position at 1.2×10^{16} cm^{-2} after a total shift of 0.22 eV. At the same time, no shift is observed in the position of the TiC signal. The total intensity of the C 1s signal decreases.

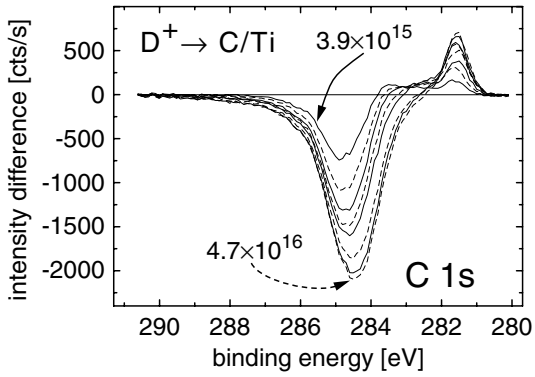

Fig. 5. XPS difference spectra after D^+ implantation in 2.9 nm carbon on Ti, in the fluence range between 3.9×10^{15} and 4.7×10^{16} cm^{-2} (difference spectra at higher fluences in Fig. 4 are omitted for clarity, since they exhibit only minor further changes). Consecutive spectra are marked with solid and broken lines, respectively. The intermediate fluence values can be taken from Fig. 4.

The graphitic peak vanishes after a D^+ fluence of 5.5×10^{16} cm^{-2}, up to where the TiC signal continually increases. Within the fluence range applied here, no complete erosion of formed TiC is observed. Compared to the spectra of the bombarded HOPG samples, no increased intensity around 285.2 eV due to ion-beam-induced effects is visible.

These observed changes in the C 1s signals are more clearly visible in the difference spectra (plotted in Fig. 5). Shown is the difference of the unirradiated spectrum from the spectra observed after fluences of 3.9×10^{15}–4.7×10^{16} cm^{-2}. Compared to HOPG in Figs. 1 and 3 where a peak in the differences around 285 eV is observed, here only an intensity decrease is visible. No additional intensity is produced by the D^+ ion beam. In contrast to Ar^+ bombardment experiments of carbon films on Ti (not shown here) where the disordered graphitic carbon (peak at 285.2 eV), produced during the carbon vapor deposition, is eroded during the first ion implantation steps, no peak is formed at this BE under D^+ bombardment.

The peak around 283.8 eV, well developed in the HOPG experiments, is also identified on the C film. However, the maximum is only distinct at the 3.9×10^{15} cm^{-2} fluence; at higher ion fluences it vanishes. The 281.8 eV peak originating from carbon in a TiC environment is clearly observed and remains fixed for all fluences. The carbide intensity continues to increase with fluence, while the total carbon intensity decreases. Intensity pointing to the existence of titanium subcarbides (around 282.6 eV) is visible at the initial stages of D^+ bombardment. After 1.6×10^{16} cm^{-2} the subcarbides are hardly discernible in the difference spectra. However, in the raw spectra (Fig. 4) there is still intensity around this

BE. The existence of subcarbides therefore cannot be excluded.

4. Discussion

During deuterium and argon ion bombardment of HOPG a shift in BE and a broadening of the C 1s peak are observed. The shift of the C 1s peak to lower BE for both ion species is caused by a decrease in intensity at the graphitic carbon position (284.2 eV) and an increase of intensity at lower BE. The difference spectra reveal a peak 0.35–0.53 eV below the graphitic signal. In contrast to the existing literature the difference spectra allow to distinguish components in the C 1s signal rather than to characterize spectral changes through mere peak shifts. Compared to results from earlier work we are able to attribute the main peak and the high-BE signal to graphitic carbon and carbon in a disordered graphitic environment [9]. The fact that the high-BE component (285.2 eV) also disappears in the HOPG experiments under annealing corroborates the assignment to a disordered graphite state. The new peak at lower BE is assigned to states induced by the ion beams. A shift to lower BE has previously been observed in the literature [15,16] without separating components in the C 1s signal. In our measurements we do not observe a shift towards higher BEs after extended ion implantation. On the contrary, after annealing of the implanted samples the C 1s signal shifts even further to lower BE.

The intensity decrease in the C 1s signal during ion implantation into HOPG is explained by the dilution of the carbon in the XPS information depth by hydrogen or argon. In contrast to what has been reported in the literature [15–17] we do not observe a peak shift to higher BEs at prolonged D^+ implantation; this shift has been attributed to the formation of C–H bonds [16,17]. BEs above 285.0 eV could also be attributed to sp^3-hybridized carbon [18] which, however, is unlikely to be produced within a collision cascade at low fluences. Not compatible with the argument of C–H bond formation for a signal at any new BE is the fact that all shifts/contributions observed here appear under both D^+ and inert Ar^+ bombardment. An interpretation of the shift to lower BEs by C–H bond formation of unsaturated hydrocarbons would be the BE values for sp and sp^2 carbon from [18]. HREELS measurements also indicate the formation of sp^2 and sp^3 carbon [19]. However, the identical observations for Ar^+ implantation rule out this interpretation at least as far as being the only explanation. Similar shifts were also observed under He^+ implantation [20]. We therefore attribute the C 1s intensity below 284.0 eV to defects in the graphite lattice, produced by the collision cascades, and therefore different from the disordered graphitic carbon with a BE of 285.2 eV. The reason for the smaller changes at below 284 eV in the case of the carbon film compared to the HOPG is the lower degree of structural order in the film. The film C 1s peak is initially already much wider than from HOPG and changes due to the ion-beam-induced effects are harder to detect.

The C 1s spectra and also the respective difference spectra of the carbon film on titanium do not allow a similar distinction between the elementary carbon binding states as in the case of HOPG. Initially, the disordered graphite phase has a high weight within the whole peak. The D^+ bombardment leads to an erosion, preferentially of the disordered graphite, and finally also of the graphitic carbon. The preferential erosion of the disordered phase is concluded from the decrease of the full-width-at half-maximum of the high-BE peak (1.63 eV initially and 1.04 eV after 3.9×10^{16} cm^{-2}), the total shift of the peak to lower BEs, as well as from the asymmetric development of the peak in the difference spectrum. As in the HOPG experiments, the D^+ bombardment leads to the formation of a small amount of radiation-induced defects, visible by the small peak around 283.6 eV in the difference spectra. In contrast to the HOPG samples, these defects in the film are only visible initially and are obscured by the decrease of the subcarbide phases during D^+ implantation. Carbon bound directly to titanium in TiC is initially present at the interface between the carbon layer and the substrate [6], and becomes more accessible to XPS with progressing layer erosion and even increases by ion-beam mixing. Ion-beam-induced carbide formation was already observed for noble gas ions [11]. After a maximum of the TiC signal (at 281.8 eV) at 5.5×10^{16} cm^{-2} this intensity decreases because of TiC erosion.

The total C 1s intensity decreases exponentially up to a fluence of 8×10^{16} cm^{-2}. Above, the intensity decrease follows a linear shape. The threshold between the two parts is characterized by the complete disappearance of carbon intensity other than from TiC (peak at 281.8 eV). The different slopes suggest different erosion mechanisms. Below the threshold, elementary carbon is eroded chemically by deuterium ions. The exponential shape is caused by an erosion mechanism which involves the entire carbon layer, similar to the ion-induced desorption of an adsorbed monolayer [21]. This is plausible since the implantation range of 4 keV D^+ in C on Ti extends to more than 100 nm, as calculated by TRIDYN. Therefore, the whole carbon layer of 2.9 nm is irradiated and chemical erosion takes place simultaneously throughout the entire layer. From the exponential curve, a reaction cross-section for carbon by D^+ of $\sigma_{chem} = 4.7 \times 10^{-17}$ cm^{-2} is calculated. Above the threshold fluence, an erosion yield of 0.003 results from a linear fit to the data. This number is in the range of the physical sputtering yield: TRIDYN calculations [22] for 4 keV D^+ on graphite give a yield of 0.0074. Taking into account that TiC has a 1:1

stoichiometry, the result of this work agrees well with this TRIDYN calculation.

5. Summary

In summary, different binding states of carbon on HOPG and carbon films on titanium during the interaction with deuterium ions are identified. The difference spectra enable one to identify contributions from disordered graphitic carbon as well as from radiation-induced defects besides the graphitic carbon state. The C 1s peak shift to lower binding energies due to ion implantation is caused by an increase of the radiation-induced defects on HOPG. In carbon films, the disordered graphitic fraction is eroded preferentially, before the remaining elementary carbon reacts. An erosion cross-section for thin carbon films is determined. Carbon bound in TiC at the interface erodes by a different mechanism with a linear rate within the applied fluences. No formation of hydrocarbons by D^+ bombardment, especially with sp^3-hybridized carbon, is observed.

References

[1] G. Federici, C.H. Skinner, J.N. Brooks, J.P. Coad, C. Grisolia, A.A. Haasz, A. Hassanein, V. Philipps, C.S. Pitcher, J. Roth, W.R. Wampler, D.C. Whyte, Nucl. Fusion 41 (2001) 1967.
[2] ITER Project, Detailed Design Document, IdoMS# G 16 DDD 2 96-11-27 W.
[3] R.A. Anderl, R.A. Causey, J.W. Davis, R.P. Doerner, G. Federici, A.A. Haasz, G.R. Longhurst, W.R. Wampler, K.L. Wilson, J. Nucl. Mater. 273 (1999) 1.
[4] H. Maier, K. Krieger, M. Balden, J. Roth, ASDEX Upgrade-Team, J. Nucl. Mater. 266–269 (1999) 1003.
[5] V. Rohde, R. Neu, R. Dux, T. Härtl, H. Maier, J. Luthin, H.G. Esser, V. Philipps, ASDEX Upgrade-Team, ECA 23J (1999) 1513.
[6] Ch. Linsmeier, J. Luthin, P. Goldstraß, J. Nucl. Mater. 290–293 (2001) 25.
[7] Ch. Linsmeier, J. Roth, K. Schmid, IAEA APID Series vol. 10, in press.
[8] P. Goldstraß, K.U. Klages, Ch. Linsmeier, J. Nucl. Mater. 290–293 (2001) 76.
[9] J. Luthin, Ch. Linsmeier, Surf. Sci. 454–456 (2000) 78.
[10] J. Luthin, Ch. Linsmeier, Physica Scripta T 91 (2001) 134.
[11] J. Luthin, H. Plank, J. Roth, Ch. Linsmeier, Nucl. Instrum. and Meth. B 182 (2001) 218.
[12] W. Eckstein, Computer Simulation of Ion–Solid Interactions, Springer Series in Materials Science, vol. 10, Springer, Berlin, 1991.
[13] S. Miller, G. Berning, H. Plank, J. Roth, J. Vac. Sci. Technol. A 15 (1997) 2029.
[14] A. Jablonski, C.J. Powell, Surf. Sci. Rep. 47 (2002) 33.
[15] H. Gotoh, Fusion Technol. 6 (1984) 424.
[16] K. Ashida, K. Kanamori, K. Ichimura, M. Matsuyama, K. Watanabe, J. Nucl. Mater. 137 (1986) 288.
[17] D. Ugolini, J. Eitle, P. Oelhafen, Appl. Phys. A 54 (1992) 57.
[18] A. Fink, W. Widdra, W. Wurth, C. Keller, M. Stichler, A. Achleitner, G. Comelli, S. Lizzit, A. Baraldi, D. Menzel, Phys. Rev. B 64 (2001) 045308.
[19] M. Portail, I. Forbeaux, N. Papapeorgiou, M. Carrère, D. Roy, J.-M. Layet, Surf. Sci. 454–456 (2000) 384.
[20] K. Ashida, K. Ichimura, M. Matsuyama, K. Watanabe, J. Nucl. Mater. 128&129 (1984) 792.
[21] E. Taglauer, W. Heiland, J. Onsgaard, Nucl. Instrum. and Meth. 168 (1980) 571.
[22] W. Eckstein, C. García-Rosales, J. Roth, W. Ottenberger, Max-Planck-Institut für Plasmaphysik, Garching, IPP-Report 9/82, 1993.